THE ASTROPHYSICAL JOURNAL, 841:41 (5pp), 2017 May 20 https://doi.org/10.3847/1538-4357/aa6d7e

AstroSat/LAXPC Detection of Millisecond Phenomena in 4U 1728-34

Jai Verdhan Chauhan[1], J S Yadav[1], Ranjeev Misra[2], P C Agrawal[3], H M Antia[1], Mayukh Pahari[2], Navin Sridhar[4], Dhiraj Dedhia[1], Tilak Katoch[1], P. Madhwani[1], R K Manchanda[5], B Paul[6], and Parag Shah[1]

[1] Tata Institute of Fundamental Research, Homi Bhabha Road, Mumbai, India; jai.chauhan@tifr.res.in
[2] Inter-University Centre for Astronomy and Astrophysics, Pune 411007, India
[3] UM-DAE Center of Excellence for Basic Sciences, University of Mumbai, Kalina, Mumbai-400098, India
[4] Indian Institute of Science Education and Research, Bhauri, Bhopal 462066, India
[5] University of Mumbai, Kalina, Mumbai-400098, India
[6] Dept. of Astronomy & Astrophysics, Raman Research Institute, Bengaluru-560080, India
Received 2017 January 25; revised 2017 April 13; accepted 2017 April 13; published 2017 May 22

Abstract

The low-mass X-ray binary 4U 1728-24 was observed with *AstroSat*/LAXPC on 2016 March 8th. Data from a randomly chosen orbit of over 3 ks was analyzed for detection of rapid intensity variations. We found that the source intensity was nearly steady but, toward the end of the observation, a typical Type-1 burst was detected. Dynamical power spectrum of the data in the 3–20 keV band, reveals the presence of a kHz Quasi-Periodic Oscillation (QPO) for which the frequency drifted from ~815 Hz at the beginning of the observation to about 850 Hz just before the burst. The QPO is also detected in the 10–20 keV band, which was not obtainable by earlier *RXTE* observations of this source. Even for such a short observation with a drifting QPO frequency, the time lag between the 5–10 and 10–20 keV bands can be constrained to be less than 100 microseconds. The Type-1 burst that lasted for about 20 s had a typical profile. During the first four seconds, dynamic power spectra reveal a burst oscillation for which the frequency increased from ~361.5 to ~363.5 Hz. This is consistent with the earlier results obtained with *RXTE*/PCA, showing the same spin frequency of the neutron star. The present results demonstrate the capability of the LAXPC instrument for detecting millisecond variability even from short observations. After *RXTE* ceased operation, LAXPC on *AstroSat* is the only instrument at present with the capability of detecting kHz QPOs and other kinds of rapid variations from 3 keV to 20 keV and possibly at higher energies as well.

Key words: accretion, accretion disks – stars: neutron – X-rays: binaries – X-rays: bursts – X-rays: individual (4U 1728-34)

1. Introduction

One of the most important and lasting legacies of the *Rossi X-ray Timing Experiment* (*RXTE*) has been the discovery and characterization of millisecond phenomena in X-ray binaries (e.g., van der Klis 2000, 2006; Remillard & McClintock 2006). These include the detection of kilohertz quasi-periodic oscillations (QPO) and the coherent burst oscillation (BO) in the initial phase of Type-1 (or thermo-nuclear) bursts.

Since their discovery, which occurred soon after the launch of *RXTE*, kHz QPOs have been the subject of extensive research and discussion. The high frequency of the variability implies that the phenomena is linked to the behavior of matter in the inner edge of the accretion disk close to the neutron star surface, and hence has the promise of revealing the behavior of matter in the strong gravitational field limit. In several low-mass X-ray binaries, these QPOs have been observed in pairs and there have been several detailed studies of their occurrence and the relationship between the pairs of frequencies as well as with that of other low-frequency QPOs (e.g., Méndez et al. 1998b; van Straaten et al. 2003; Altamirano et al. 2008; Belloni et al. 2007). Attempts have been made to explain these relations with theoretically motivated models in which one of the frequencies is identified as Keplerian and the other as a result of complex interactions that may occur in such regions, such as beating of frequencies or resonances (e.g., Lamb et al. 1998; Osherovich & Titarchuk 1999; Stella & Vietri 1999). Despite these endeavors, it is perhaps fair to say that there is no consensus on which of these dynamical models represents the correct physical picture, and the underlying physical phenomena of kHz QPO remains an open question. While these studies have focused on understanding the dynamical origin of the kHz QPOs, there have been relatively less attempts on identifying the radiative processes by which the phenomena is manifested. The QPOs are known to occur at particular spectral states of the system and understanding the radiative components and specifically the spectral parameters that vary to produce the QPO, would enhance our understanding of their origin. This can be done by studying the fractional rms and time lag as a function of photon energy (e.g., Berger et al. 1996; Vaughan et al. 1997; Kaaret et al. 1999; Méndez et al. 2001; Barret 2013; de Avellar et al. 2013; Peille et al. 2015). The increase of rms with energy and soft lags can be explained in the framework of a Comptonization model and such an analysis cannot only constrain the responsible radiative process but also provide estimates of the size and geometry of the region (Lee et al. 2001; Kumar & Misra 2016).

It should be emphasized that a large fraction of the X-ray binaries are transient and the kHz QPOs are known to occur only during certain spectral states. Hence it is important to continuously monitor the X-ray sky for new X-ray binaries and to study the known ones to get new insights into the phenomena. For example, oscillations observed on timescales significantly smaller than millseconds, will revolutionize our understanding of the kHz QPOs. Thus, there is a critical need for instruments that have the capability of observing the high-frequency variations in the post-*RXTE* era.

Unlike kHz QPOs, the frequency of the coherent oscillation observed during the initial burst decay phase of a Type-1 burst, is unambiguously related to the spin of the neutron star (e.g., Strohmayer et al. 1997; Chakrabarty et al. 2003). During the initial period of a Type I burst, it is believed that uneven nuclear burning of material accreted on the surface of the neutron star, is the cause of the observed coherent burst oscillations, though the exact mechanism is not clear (e.g., Strohmayer & Markwardt 1999; Muno et al. 2004; Chakraborty & Bhattacharyya 2014). Indeed, for low-mass X-ray binaries, our knowledge of the spin period of the neutron star is solely derived from the burst oscillations. Thus, for new X-ray transients, it is important to have the capability to measure the BO and hence infer the spin period of the neutron star. The Type I bursts and the rapid oscillations are by themselves an interesting phenomenon, providing rich information about the nuclear burning process and other several not well understood features like why the oscillations persists for as long as 5–10 s. Broadband observations of these bursts and energy dependent time lags will provide crucial information to probe these processes deeper.

With an effective area similar to that of *RXTE* at low ∼5 keV and significantly larger at higher energies (∼50 keV), the Large Area X-ray Proportional Counter (LAXPC; Yadav et al. 2016a; Antia et al. 2017) on board the Indian X-ray mission, *AstroSat* (Agrawal 2006; Singh et al. 2014), is expected to detect and discover millisecond variability in X-ray binaries, leading to significant enhancement of our understanding of the phenomena. Moreover, the other instruments on board *AstroSat* will provide wide band coverage from UV to hard X-rays. LAXPC data of black-hole systems GRS 1915+105 and Cygnus X-1 have already demonstrated the capability of LAXPC to study variability of high-energy photons (Yadav et al. 2016b; Misra et al. 2017).

4U 1728-34 (GX 354-0) is a well studied atoll-type low-mass X-ray binary for which *RXTE* has detected kHz QPOs during several occasions (e.g., Strohmayer et al. 1996; Migliari et al. 2003; Mukherjee & Bhattacharyya 2012). The frequency of the lower kHz QPO covers a wide range from 300 to 1100 Hz. The source exhibits frequent Type-1 bursts for which burst oscillations have been detected at ∼363 Hz (Strohmayer et al. 1997) and extensively studied (Muno et al. 2001; van Straaten et al. 2001; Muno et al. 2004; Zhang et al. 2016). Here we report the first detection of both kHz QPO and the burst oscillation for a short ∼3 ks observation of 4U 1728-34 by *AstroSat*/LAXPC. The kHz QPO is detected in energies >10 keV, which *RXTE* was not able to do (Mukherjee & Bhattacharyya 2012), thereby convincingly demonstrating its superior capability to detect millisecond variability.

2. Detection of kHz QPO

The 1 s binned light curve generated using data from *AstroSat* orbit number 2398 during 2016 March 8th is shown in Figure 1. 4U 1728-34 was detected at a level of ∼1500 c s^{-1} and near the end of the observation there was a Type-1 burst, where the flux reached ∼10000 c s^{-1} at the peak.

Figure 2 shows the photon spectrum from one of the LAXPC units (namely LAXPC 10) for the first ∼2500 s of data. The response matrix and the background were obtained using software that would be part of the standard LAXPC pipeline and as described in Yadav et al. (2016a) and Antia et al. (2017), and a systematic uncertainty of 1% was included in the spectral fitting. The data can be reasonably modeled (χ^2/dof = 92.3/104) by an absorbed thermal Comptonization component ("Tbabs*nthcomp" in Xspec) with photon index 1.8 ± 0.02 and temperature 3.05 ± 0.04 keV and a column density of 2.2 ± 0.4 × 10^{22} cm^{-2}. A weak but broad Iron line is required for the fit. Figure 2 also shows the expected background spectrum and we note that it does not dominate until ∼20 keV. Given the spectral resolution and uncertainty in the response, the spectral shape of the source is as expected and we concentrate now on the rapid timing behavior, which is the focus of the present work.

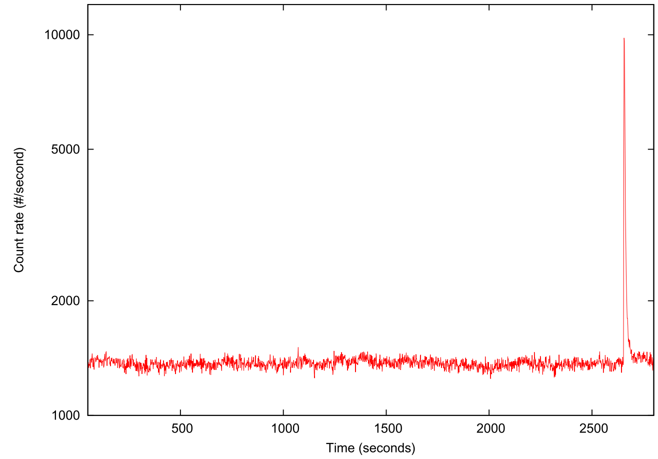

Figure 1. Light curve of 4U 1728-34 in the energy range of 3–20 keV is shown where the count rate from all three LAXPC detectors are combined.

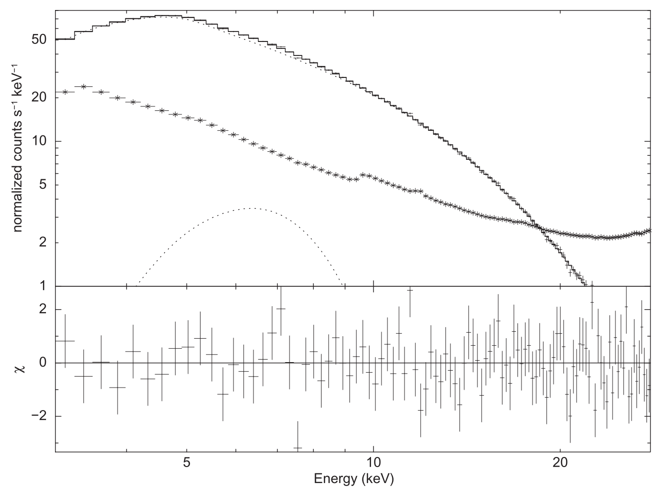

Figure 2. Photon spectrum from LAXPC 10 for the first ∼2500 s. The spectrum is modeled using a thermal Comptonization component and a broad iron line. The plot also shows the expected background spectrum.

The power spectrum for the first 2500 s showed evidence for features around ∼800 Hz, which suggested the presence of a drifting kHz QPO. This was confirmed using dynamic power spectra analysis; the results of which are shown in the top panel of Figure 3. The dynamic power spectra were created by splitting the 3–20 keV light curve into 16 parts of 147.97 s each. Each part was then divided into 289 segments of 0.512 s. The power spectra have been normalized such that the Poisson level, P_N is at 2, i.e., they are "Leahy" normalized (Leahy et al. 1983). The ∼40 microsecond dead-time of the instrument reduces the noise level slightly to ∼1.95. Power spectra were created for each of the 289 segments and averaged. Hence, the error on the power at each frequency, $\Delta P/P$ is $1/\sqrt{(N)} = 1/\sqrt{(289)}$ or 5.9%. The middle panel of Figure 3 shows the significance $\sigma \equiv (P - P_N)/\Delta P$ for the detections.

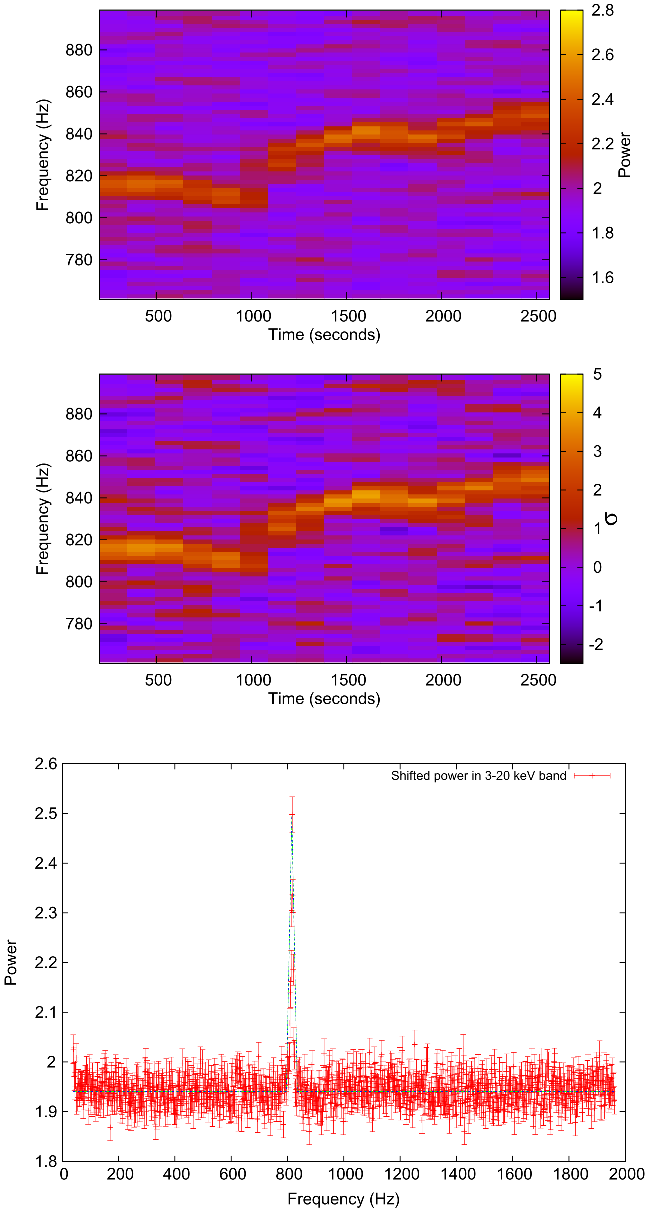

Figure 3. Dynamic power spectra of 4U 1728-34 in the energy range of 3–20 keV (top panel). A drifting kHz QPO whose frequency changes from ∼815 Hz to ∼850 Hz is clearly visible. The middle panel shows the variation of $\sigma \equiv (P - P_n)/\Delta P$ showing that the QPO is significantly detected. The bottom panel shows the co-added power spectra after aligning the QPO frequency. No other features are detected in the 200–2000 Hz.

The figures clearly reveal a significant QPO whose frequency drifts from ∼815 Hz at the beginning of the observation to ∼850 toward the end. To explore the possibility of any other QPO in the data, we used the standard shift and add technique, where the power spectrum for each part is shifted such that the QPO frequencies become aligned and then averaged (Méndez et al. 1998a; Mukherjee & Bhattacharyya 2012). The resultant power spectrum is shown in the bottom panel of Figure 3, which shows no other QPO-like features.

We test whether the kHz QPO is also detected at high energies (>10 keV), especially since earlier *RXTE* analysis of the source was unable to do so (Mukherjee & Bhattacharyya 2012). Power spectra were computed in the 10–20 keV band and following Mukherjee & Bhattacharyya (2012), the spectra for each part were shifted in frequency using the QPO detected

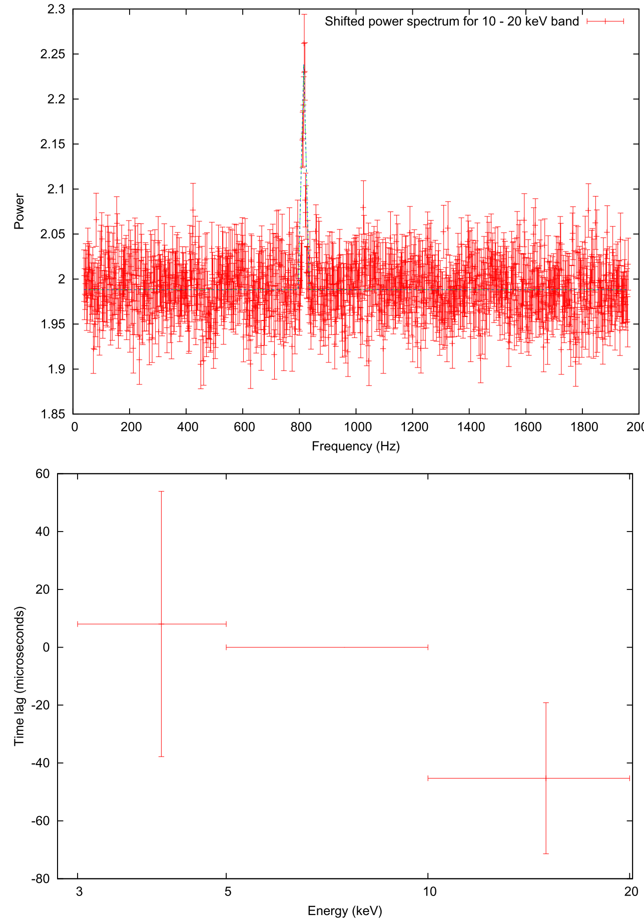

Figure 4. Time lag as a function of energy for the kHz QPO. The reference band here is 5–10 keV. Even for the short duration of ∼2500 s data the time lag can be constrained to <100 microseconds.

in the 3–20 keV spectra as the reference. The averaged spectrum is shown in the top panel of Figure 4 and the khz QPO is clearly detected in the high-energy band. Fitting the power spectrum with a Gaussian and a constant component gives $\chi^2/\mathrm{dof} = 991.2/982$, while only a constant component gives 1231.8/984 or a $\Delta\chi^2 = 240$ for two additional degrees of freedom.

One does not expect to obtain tight constrains on energy dependent time lag from such a short duration data, especially when the frequency of the QPO is drifting. Nevertheless, the detection of the QPO in high-energy bands allows the computation of energy dependent time-lags as shown in Figure 4. The time lag was computed from the shift and added averaged cross-spectra as described for the power spectra above and its error was estimated using the method described in Nowak et al. (1999). Since the length of each segment is 0.512 s, the frequency resolution Δf of the cross-spectra is ∼1.98 Hz. We have verified that changing this resolution to ∼4 or ∼1 Hz does not change the results obtained. The time lag is constrained to be less than 100 microseconds, which indicates the capabilities of the LAXPC to undertake such an analysis with larger or better quality observations.

3. Detection of Burst Oscillations

Figure 5 shows the light curve of the Type-1 burst at a finer time resolution of 0.128 s. The burst profile is typical with a

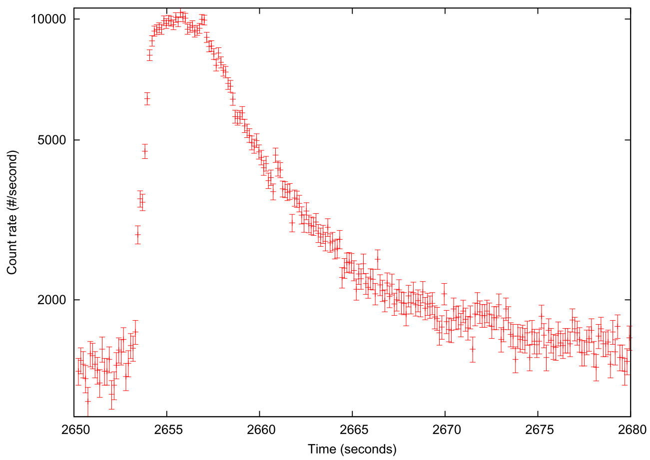

Figure 5. Light curve of the Type I X-ray burst observed in 4U 1728-34 in the energy range of 3–20 keV. The count rates from all three LAXPC detectors are combined, and the time bin is 0.128 s.

fast rise and slower decay lasting for about 20 s. Since burst oscillations are often detected in the early phase of the burst, we looked for high-frequency signatures in the first 5 s of the burst by computing the dynamic power spectra. The first 5.12 s of the burst was divided into 10 parts and the power spectra were computed for each of them to get the dynamic power spectra as shown in the top panel of Figure 6. A coherent feature is observed at 362 Hz, which is referred to as the burst oscillation. The power spectra are "Leahy" normalized and each one is computed from one segment. Thus the null hypothesis probability that a power as high as observed is obtained by chance is $N_f e^{(-P(f)/2)}$ (e.g., Vaughan et al. 1994), where N_f is the number of independent frequencies being considered. Since we were searching for oscillations <1000 Hz at a frequency resolution of $\sim$2 Hz, we chose $N_f = 500$. The maximum value of $P(f)$ is $\sim$34, which implies a null hypothesis probability of 2×10^{-5}. Thus the oscillation is detected at a high level of significance. The bottom panel of Figure 6 shows a more close-up view of the dynamic power spectra represented by a contour map. The burst oscillation frequencies increase from $\sim$361.5 to $\sim$363.5 Hz, which has been reported earlier using *RXTE* for this and other sources (e.g., Watts 2012 and references therein).

4. Discussion

We have presented here the first detection of both kinds of millisecond variability, i.e., kHz QPOs and burst oscillation in the LMXB 4U 1728-34 with *AstroSat*/LAXPC from a single $\sim$3 ks observation. This result demonstrates that the LAXPC instrument has the necessary sensitivity and time resolution to detect and study millisecond timing phenomena in 3–20 keV and possibly at higher energy as well.

With *RXTE*, there have been relatively few studies of the high-frequency QPOs at energy 20 keV mainly due to rapid decline in the effective of PCA at higher energies. In fact, detailed energy dependence of both the fractional rms and time lag for kHz QPO have been possible for only one or two orbits of *RXTE* observations, i.e., the 1996 March 3rd observation of 4U 1608-52 (Berger et al. 1996; Vaughan et al. 1997) and 1998 February 24 and 1996 April 27 observations of 4U 1636-53 (Zhang et al. 1996; Kaaret et al. 1999). Barret (2013), de Avellar et al. (2013), and Peille et al. (2015) had to combine a large number of *RXTE* observations to obtain average energy dependent rms and time lag for different QPO frequency ranges. During its latter stage, *RXTE* observations were undertaken with only one or two of its five PCUs, hence making significant detections in short observations harder. For example, for the source analyzed in this work, 4U 1728-34, the QPO was not detected in the 10–20 keV band even when 85 ks were analyzed (Mukherjee & Bhattacharyya 2012). In contrast, the 3 ks LAXPC data detected the QPO in the band as shown in the dynamic power spectrum (Figure 3). Thus *AstroSat*/LAXPC has now proven the potential to study the energy dependence of kHz QPO. A critical advantage will be obtained by the simultaneous observations from other instruments on board *AstroSat*, especially the Soft X-ray Telescope (SXT). The broadband coverage will measure more accurately the time-averaged radiative components of the system thereby having significantly more constrains. For example, using *RXTE* observations, the spectral modeling was degenerate leading to ambiguities regarding the size and geometry of the source as inferred from the energy dependent properties of the kHz QPO (Kumar & Misra 2016). The SXT spectra in the 0.3–8 keV band will lift this degeneracy allowing one to test different models and to obtain interesting physical constraints such as size and geometry of the source.

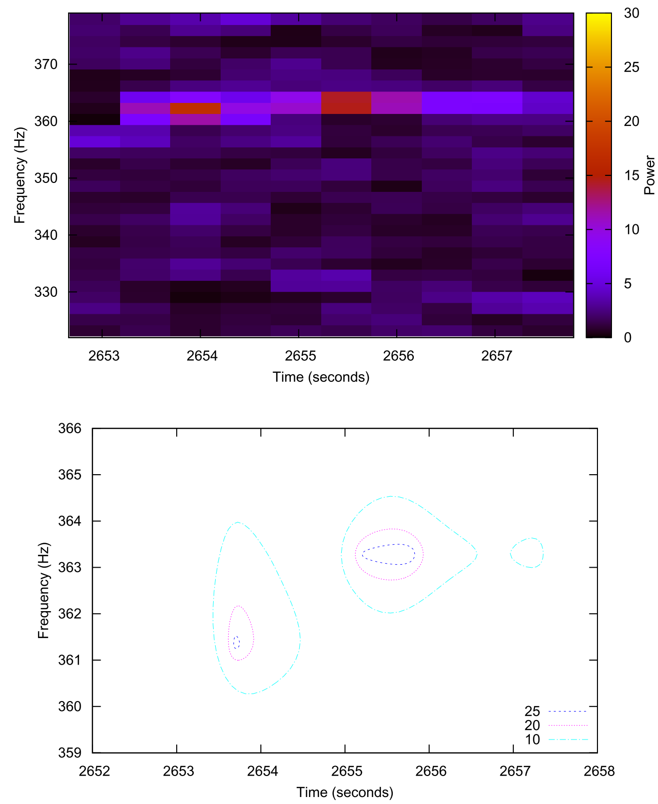

Figure 6. Dynamic power spectra of the first 5 s of the Type-1 burst shown in the color map (top panel) and contour representation (bottom panel). The power spectrum are "Leahy" normalized and the contour lines are drawn for power values of 10, 20, and 25. A coherent feature at 363 Hz is seen.

Confirmation of the 363 Hz burst oscillation of the source brings out the potential of LAXPC to detect the phenomena and, in general, to enhance our understanding of Type-1 bursts. *AstroSat* will also enable the broadband study of the spectral evolution of the burst using LAXPC and SXT. Of particular interest could be the measurement of time delays between the

X-rays and the UV emission as detected by the Ultra-Violet Imaging Telescope (UVIT). These delays correspond to the light crossing time to the outer disk and provide constrains on the disk geometry (e.g., Hynes et al. 2006).

We defer detailed analysis and interpretation of the data to later works where the properties of the kHz QPO and burst oscillations will be studied separately. Our first look results show with confidence that the *RXTE* legacy of studying millisecond variability of X-ray binaries will be effectively carried forward by *AstroSat* and one can look forward to new exciting discoveries in the near future.

We acknowledge the strong support from Indian Space Research Organization (ISRO) in various aspects of instrument building, testing, software development, and mission operation during payload verification phase. We acknowledge support of the scientific and technical staff of the LAXPC team as well as staff of the TIFR Workshop in the development and testing of the LAXPC instrument.

References

Agrawal, P. C. 2006, AdSpR, 38, 2989
Altamirano, D., van der Klis, M., Méndez, M., et al. 2008, ApJ, 685, 436
Antia, H. M., Yadav, J. S., Agrawal, P. C., et al. 2017, arXiv:1702.08624
Barret, D. 2013, ApJ, 770, 9
Belloni, T., Méndez, M., & Homan, J. 2007, MNRAS, 376, 1133
Berger, M., van der Klis, M., van Paradijs, J., et al. 1996, ApJL, 469, L13
Chakrabarty, D., Morgan, E. H., Muno, M. P., et al. 2003, Natur, 424, 42
Chakraborty, M., & Bhattacharyya, S. 2014, ApJ, 792, 4
de Avellar, M. G. B., Méndez, M., Sanna, A., & Horvath, J. E. 2013, MNRAS, 433, 3453
Hynes, R. I., Horne, K., O'Brien, K., et al. 2006, ApJ, 648, 1156
Kaaret, P., Piraino, S., Ford, E. C., & Santangelo, A. 1999, ApJL, 514, L31
Kumar, N., & Misra, R. 2016, MNRAS, 461, 2580
Lamb, F. K., Miller, M. C., & Psaltis, D. 1998, NuPhB, 69, 113
Leahy, D. A., Elsner, R. F., & Weisskopf, M. C. 1983, ApJ, 272, 256
Lee, H. C., Misra, R., & Taam, R. E. 2001, ApJL, 549, L229
Méndez, M., van der Klis, M., & Ford, E. C. 2001, ApJ, 561, 1016
Méndez, M., van der Klis, M., van Paradijs, J., et al. 1998a, ApJL, 494, L65
Méndez, M., van der Klis, M., Wijnands, R., et al. 1998b, ApJL, 505, L23
Migliari, S., van der Klis, M., & Fender, R. P. 2003, MNRAS, 345, L35
Misra, R., Yadav, J. S., Verdhan Chauhan, J., et al. 2017, ApJ, 835, 195
Mukherjee, A., & Bhattacharyya, S. 2012, ApJ, 756, 55
Muno, M. P., Chakrabarty, D., Galloway, D. K., & Savov, P. 2001, ApJL, 553, L157
Muno, M. P., Galloway, D. K., & Chakrabarty, D. 2004, ApJ, 608, 930
Nowak, M. A., Vaughan, B. A., Wilms, J., Dove, J. B., & Begelman, M. C. 1999, ApJ, 510, 874
Osherovich, V., & Titarchuk, L. 1999, ApJL, 522, L113
Peille, P., Barret, D., & Uttley, P. 2015, ApJ, 811, 109
Remillard, R. A., & McClintock, J. E. 2006, ARA&A, 44, 49
Singh, K. P., Tandon, S. N., Agrawal, P. C., et al. 2014, Proc. SPIE, 9144, 91441S
Stella, L., & Vietri, M. 1999, PhRvL, 82, 17
Strohmayer, T. E., & Markwardt, C. B. 1999, ApJL, 516, L81
Strohmayer, T. E., Zhang, W., Swank, J. H., et al. 1996, ApJL, 469, L9
Strohmayer, T. E., Zhang, W., & Swank, J. H. 1997, ApJL, 487, L77
van der Klis, M. 2000, ARA&A, 38, 717
van der Klis, M. 2006, AdSpR, 38, 2675
van Straaten, S., van der Klis, M., Kuulkers, E., & Méndez, M. 2001, ApJ, 551, 907
van Straaten, S., van der Klis, M., & Méndez, M. 2003, ApJ, 596, 1155
Vaughan, B. A., van der Klis, M., Méndez, M., et al. 1997, ApJL, 483, L115
Vaughan, B. A., van der Klis, M., Wood, K. S., et al. 1994, ApJ, 435, 362
Watts, A. L. 2012, ARA&A, 50, 609
Yadav, J. S., Agrawal, P. C., Antia, H. M., et al. 2016a, Proc. SPIE, 9905, 99051D
Yadav, J. S., Misra, R., Verdhan Chauhan, J., et al. 2016b, ApJ, 833, 27
Zhang, W., Lapidus, I., White, N. E., & Titarchuk, L. 1996, ApJL, 469, L17
Zhang, G., Méndez, M., Zamfir, M., & Cumming, A. 2016, MNRAS, 455, 2004